

Piezoelectric-based Vibration Control in Composite Structures

J L Cao¹, S John¹, and T Molyneux²

¹School of Aerospace, Mechanical & Manufacturing Engineering, RMIT University
Bundoora East Campus, PO Box 71, Bundoora, VIC 3083, Australia.

E-mail: sabu.john@rmit.edu.au

²School of Civil & Chemical Engineering, RMIT University
City Campus, GPO Box 2476V, Melbourne, VIC 3001, Australia.

E-mail: tom.molyneux@rmit.edu.au

1 Abstract

This paper relates to vibration control using passive electrical shunt circuits. However, the vibration shunt control efficiency relies on the optimization of the vibration energy transfer between a structure and a Lead-Zirconate-Titanate (PZT) piezoelectric ceramic material. The problem is further complicated by the material composition of the substrate or host material the PZT is coupled to. In this paper, an analytical study of a parallel resistor-inductor piezoelectric vibration shunt control on a composite beam structure is presented. The influence of the geometry size and material property on the mechanical strain produced in the PZT is discussed.

Keywords: Composite, Vibration, Strain Energy, Piezoelectric, Shunt Circuit.

2 Introduction

Structural vibration control has been a subject of engineering research for the past few decades. Recently, the use of "smart" materials for vibration control has become an alternative to traditional vibration control techniques. Vibration control with "smart" materials has several advantages such as lighter weight, smaller size, flexibility in the structure and lower cost. They are especially suitable where the traditional techniques cannot be applied due to weight and size restrictions.

The smart material components such as Lead-Zirconate-Titanate (PZT), a piezoelectric ceramic material, can convert mechanical energy into electrical energy and vice versa. Hagood and von Flotow (1991) have demonstrated that the vibrations of the structure can be damped with piezoelectric materials and a passive electrical (shunt) network [1]. The piezoelectric materials convert vibration energy into electrical energy and then dissipate the electrical energy in the form of joule heating through the passive electrical (shunt) network, which is also known as passive vibration damping.

The electrical (shunt) network consists of resistors, capacitors and inductors. The network is connected across a PZT transducer, which can be modeled as a strain controlled voltage source in series with an inherent capacitance, or a strain controlled current source in parallel with the inherent capacitance. The PZT transducer can alter the stiffness and loss factor of the system to be attached. It acts as a Tuned Mass Damper (TMD) or tuned vibration absorber (TVA).

It is widely reported [1 ~ 6] that significant amount of vibration be removed when resistor-inductor (RL) or resistor-inductor-capacitor (RLC) shunt circuits are optimally tuned.

To maximize the vibration energy to be shunted by the PZT, it is preferred to transfer more energy from a structure onto the PZT. Simulation and experimental results have shown that the material property of the structure affects the energy transfer between the structure and the PZT.

3 Equation of motion of a composite beam

"Piezoelectric effect" is that when a crystal is under pressure, an electrical potential appears across some of its faces (direct effect). When an electrical field is applied, mechanical deformation of the crystal occurs (converse effect). The most common material possesses the "Piezoelectric effect" is Lead-Zirconium-Titanium (PZT). The "Piezoelectric effect" indicates that there is energy conversion or transduction from one form to another occurring during the deformation process. For passive vibration shunting with piezoelectric material, "direct effect" is used.

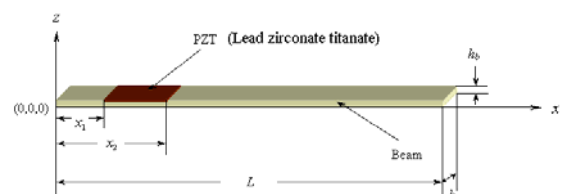


Figure 1 PZT attached to the composite beam

Figure 1 is a cantilever beam with a PZT patch attached, sometimes called as a composite beam. The motion equation of the composite beam under pure bending can be derived as

$$\begin{aligned}
& E_b I_b \frac{\partial^4 w}{\partial x^4} + E_p I_p \frac{\partial^4 w}{\partial x^4} [H(x-x_1) - H(x-x_2)] + \\
& 2E_p I_p \frac{\partial^3 w}{\partial x^3} [\delta(x-x_1) - \delta(x-x_2)] + \\
& E_p I_p \frac{\partial^2 w}{\partial x^2} [\delta'(x-x_1) - \delta'(x-x_2)] + \\
& \rho_b A_b \frac{\partial^2 w}{\partial t^2} + \rho_p A_p \frac{\partial^2 w}{\partial t^2} [H(x-x_1) - H(x-x_2)] - \\
& h_{31} A_p (h_b + \frac{h_p}{2}) D_3 [\delta'(x-x_1) - \delta'(x-x_2)] = f(x,t) \quad (1)
\end{aligned}$$

with boundary conditions:

$$\begin{cases} E_b I_b \frac{\partial^2 w}{\partial x^2} \delta \left(\frac{\partial w}{\partial x} \right) \Big|_0^L = 0 \Rightarrow \frac{\partial^2 w}{\partial x^2} = 0 \text{ or } \delta \left(\frac{\partial w}{\partial x} \right) = 0 \\ E_b I_b \frac{\partial^3 w}{\partial x^3} \delta w \Big|_0^L = 0 \Rightarrow \frac{\partial^3 w}{\partial x^3} = 0 \text{ or } \delta w = 0 \end{cases} \quad (2)$$

where

w — Transverse displacement of composite beam

h_b — Thickness of beam

h_p — Thickness of PZT

$A_p = bh_p$ — Cross-sectional area of PZT

$A_b = bh_b$ — Cross-sectional area of beam

I_b — Area moment of inertia of beam about the neutral axis

I_p — Area moment of inertia of PZT about the neutral axis

E_b — Elastic modulus of beam

E_p — Elastic modulus of PZT

ρ_b — Density of beam

ρ_p — Density of PZT

D_3 — Electrical displacement in “3” direction

$H(x)$ — Heavyside function

$\delta(x)$ — Dirac-delta function

4 Composite beam with parallel R-L shunt networks.

According to mode separation method

$$w(x,t) = \sum_{r=1}^{\infty} \phi_r(x) q_r(t) \approx \sum_{r=1}^N \phi_r(x) q_r(t) \quad (3)$$

where $\phi_r(x)$ satisfies all the boundary condition.

Substitute equation (3) into equation (1), using Galerkin’s method, the partial differential equation of equation (1) can be discretized into an ordinary differential equation as shown below

$$\begin{aligned}
& \sum_{r=1}^N \left(\int_0^L [\rho_b A_b + \rho_p A_p [H(x-x_1) - H(x-x_2)]] \phi_r(x) \phi_s(x) dx \right) \ddot{q}_r(t) + \\
& \sum_{r=1}^N \left(\int_0^L [E_b I_b + E_p I_p [H(x-x_1) - H(x-x_2)]] \phi_r''(x) \phi_s''(x) dx \right) q_r(t) \\
& - \frac{h_{31} A_p}{\beta_{33}} (h_b + \frac{h_p}{2}) D_3 \int_{x_1}^{x_2} \phi_s''(x) dx = \int_0^L f(x,t) \phi_s(x) dx \quad (4)
\end{aligned}$$

where,

$$D_3 = \frac{1}{\beta_{33}} (E_3 + h_{31} \varepsilon_{11}) = \frac{1}{\beta_{33}} \left(\frac{v(t)}{h_p} + h_{31} \varepsilon_{11} \right) \quad (5)$$

E_3 is the electrical field of the PZT in “3” direction

$\varepsilon_{11} = -z \frac{\partial^2 w}{\partial x^2}$ is the axial strain in x direction

β_{33} is the electrical impermeability of PZT in “3-3” direction

h_{31} is the electrical displacement-stress coefficient of PZT in “3-1” direction

$v(t)$ is the voltage across the PZT patch

When a parallel RL shunt circuit is connected across the electrodes of the PZT, the electrical current due to electrical charge generated from the mechanical stress flows to the RL shunt circuit. According to Kirchhoff’s laws, this is:

$$\begin{aligned}
i(t) &= -\frac{dQ}{dt} = -S_p \frac{dD_3}{dt} \\
&= -C_p \frac{dv(t)}{dt} - h_{31} h_p C_p \frac{d\varepsilon_{11}}{dt} = i_L(t) + i_R(t) \quad (6)
\end{aligned}$$

Equation (6) can be rewritten as

$$i_C + i_L + i_R = -I_S \quad (7)$$

where

$i_C = C_p \frac{dv}{dt}$ is electrical current in $C_p = \frac{S_p}{\beta_{33} h_p}$,

i_L and i_R are electrical currents in the inductor and resistor of shunt circuit respectively, $I_S = h_{31} h_p C_p \frac{d\varepsilon_{11}}{dt}$

is the electrical current generated due to the mechanical stress.

The circuit model of the equation (7) is depicted in Figure 2 that represents the parallel RL shunt circuit.

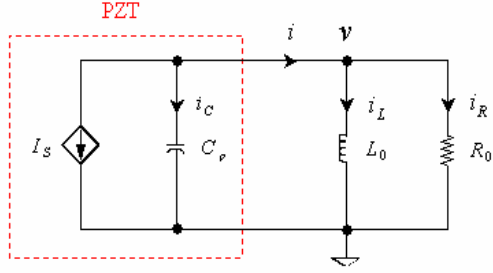


Figure 2 Equivalent circuit of parallel RL shunt

The voltage $v(t)$ can be obtained from,

$$\begin{aligned} v(t) &= \frac{1}{C_p} \int i_C dt = -\frac{1}{C_p} \int \left(h_{31} h_p C_p \frac{d\varepsilon_{11}}{dt} + i_R + i_L \right) dt \\ &= -\frac{1}{C_p} \int \left(h_{31} h_p C_p \frac{d\varepsilon_{11}}{dt} + \frac{L_0}{R_0} \frac{di_L}{dt} + i_L \right) dt \\ &= -h_{31} h_p \varepsilon_{11} - \frac{L_0}{R_0 C_p} i_L - \frac{1}{C_p} \int i_L dt \end{aligned} \quad (8)$$

Substituting equation (8) into equation (5),

$$D_3 = -\frac{1}{\beta_{33} h_p} \left(\frac{L_0}{R_0 C_p} i_L + \frac{1}{C_p} \int i_L dt \right) \quad (9)$$

Then equation (4) then becomes,

$$\begin{aligned} &\sum_{r=1}^N \left(\int_0^L [\rho_b A_b + \rho_p A_p [H(x-x_1) - H(x-x_2)]] \phi_r(x) \phi_s(x) dx \right) \ddot{q}_r(t) + \\ &\sum_{r=1}^N \left(\int_0^L [\rho_b A_b + \rho_p A_p [H(x-x_1) - H(x-x_2)]] \phi_r(x) \phi_s(x) dx \right) \ddot{q}_r(t) \\ &+ B_L i_L + B_R \int i_L dt = \int_0^L f(x, t) \phi_s(x) dx \end{aligned} \quad (10)$$

where,

$$B_L = h_{31} \left(h_b + \frac{h_p}{2} \right) \frac{L_0}{R_0} [\phi_s'(x_2) - \phi_s'(x_1)] \quad (11)$$

$$B_R = h_{31} \left(h_b + \frac{h_p}{2} \right) [\phi_s(x_2) - \phi_s(x_1)] \quad (12)$$

On the other hand, since $v(t) = L_0 \frac{di_L}{dt}$, combining this with equation (8),

$$L_0 \frac{di_L}{dt} = -h_{31} h_p \varepsilon_{11} - \frac{L_0}{R_0 C_p} i_L - \frac{1}{C_p} \int i_L dt$$

Or,

$$L_0 \frac{di_L}{dt} + \frac{L_0}{R_0 C_p} i_L + \frac{1}{C_p} \int i_L dt = h_{31} h_p z \frac{\partial^2 w}{\partial x^2} \quad (13)$$

where strain ε_{11} has been replaced by $-z \frac{\partial^2 w}{\partial x^2}$.

Integrating both side of equation (13) to eliminate variable z and considering equation

$$\frac{\partial^2 w}{\partial x^2} = \left(\sum_{r=1}^N \phi_r''(x) \right) q_r(t),$$

$$\int_{h_b}^{h_b+h_p} \left(L_0 \frac{di_L}{dt} + \frac{L_0}{R_0 C_p} i_L + \frac{1}{C_p} \int i_L dt \right) dz = h_{31} h_p \int_{h_b}^{h_b+h_p} z \frac{\partial^2 w}{\partial x^2} dz$$

one can have

$$\frac{di_L}{dt} + \frac{1}{R_0 C_p} i_L + \frac{1}{L_0 C_p} \int i_L dt + \sum_{r=1}^N \psi_r q_r = 0 \quad (14)$$

Equation (14) represents piezoelectric vibration control with a single parallel R-L shunt circuit. In general, multiple parallel R-L shunt control can be represented as matrix form (assume each control circuit is mutual non-interference), The matrix form of equation (14) is

$$\dot{\mathbf{i}}_L + \mathbf{\Gamma} \mathbf{i}_L + \mathbf{\Omega} \tilde{\mathbf{i}}_L + \mathbf{\Psi} \mathbf{q} = \mathbf{0} \quad (15)$$

where

$$\mathbf{i}_L = [i_{L1} \ \dots \ i_{LN}]_{N \times 1}^T, \quad \tilde{\mathbf{i}}_L = \int \mathbf{i}_L dt, \quad \dot{\mathbf{i}}_L = \frac{d\mathbf{i}_L}{dt}$$

$$\mathbf{\Gamma} = \begin{bmatrix} \frac{1}{C_p R_1} & & 0 \\ & \ddots & \\ 0 & & \frac{1}{C_p R_N} \end{bmatrix}, \quad \mathbf{\Omega} = \begin{bmatrix} \frac{1}{C_p L_1} & & 0 \\ & \ddots & \\ 0 & & \frac{1}{C_p L_N} \end{bmatrix},$$

$$\mathbf{\Psi} = \begin{bmatrix} \psi_1 & & 0 \\ & \ddots & \\ 0 & & \psi_N \end{bmatrix}$$

$$\psi_r = -\frac{h_{31} h_p (2h_b + h_p)}{2(x_2 - x_1) L_0} \int_{x_1}^{x_2} \phi_r''(x) dx \quad (r = 1, \dots, N)$$

The equation (10) can be written is a concise form as,

$$\sum_{r=1}^N m_{sr} \ddot{q}_r + \sum_{r=1}^N k_{sr} q_r + B_L i_L + B_R \int i_L dt = f_d(t) \quad (16)$$

The matrix form of equation (16) is,

$$\mathbf{M} \ddot{\mathbf{q}} + \mathbf{K} \mathbf{q} + \mathbf{B}_L \mathbf{i}_L + \mathbf{B}_R \tilde{\mathbf{i}}_L = \mathbf{f}_d \quad (17)$$

where

$$\mathbf{M} = \begin{bmatrix} m_{11} & \dots & m_{1N} \\ \vdots & \ddots & \vdots \\ m_{N1} & \dots & m_{NN} \end{bmatrix}, \quad \mathbf{K} = \begin{bmatrix} k_{11} & \dots & k_{1N} \\ \vdots & \ddots & \vdots \\ k_{N1} & \dots & k_{NN} \end{bmatrix},$$

$$\mathbf{B}_L = \begin{bmatrix} B_1^L & & 0 \\ & \ddots & \\ 0 & & B_N^L \end{bmatrix}, \quad \mathbf{B}_R = \begin{bmatrix} B_1^R & & 0 \\ & \ddots & \\ 0 & & B_N^R \end{bmatrix},$$

$$\mathbf{f}_d = \begin{bmatrix} f_{d1} \\ \vdots \\ f_{dN} \end{bmatrix}_{N \times 1}.$$

$$m_{sr} = \int_0^L [\rho_b A_b + \rho_p A_p [H(x-x_1) - H(x-x_2)]] \phi_r(x) \phi_s(x) dx$$

$$k_{sr} = \int_0^L [E_b I_b + E_p I_p [H(x-x_1) - H(x-x_2)]] \phi_r''(x) \phi_s''(x) dx$$

$$f_d = \int_0^L f(x,t) \phi_s(x) dx = \int_0^L F_d(t) \delta(x-x_d) \phi_s(x) dx,$$

(x_d is where force applied and response measured)

$$B_S^L = \frac{h_{31} h_p (2h_b + h_p)}{2(x_2 - x_1)} \frac{L_S}{R_S} \int_{x_1}^{x_2} \phi_s''(x) dx$$

(R_S and L_S are shunt resistor and inductor respectively, $s = 1, \dots, N$)

$$B_S^R = \frac{h_{31} h_p (2h_b + h_p)}{2(x_2 - x_1)} \int_{x_1}^{x_2} \phi_s''(x) dx \quad (s = 1, \dots, N)$$

When considering internal structural damping, equation (17) can be extended to

$$\mathbf{M}\ddot{\mathbf{q}} + \mathbf{C}\dot{\mathbf{q}} + \mathbf{K}\mathbf{q} + \mathbf{B}_L \dot{\mathbf{i}}_L + \mathbf{B}_R \tilde{\mathbf{i}}_L = \mathbf{f}_d \quad (18)$$

where

$\mathbf{C} = \alpha \mathbf{M} + \gamma \mathbf{K}$ — the Rayleigh damping coefficient, α and γ are constants.

Convert equations (15 & 18) to state space form as

$$\begin{aligned} \dot{\mathbf{x}} &= \mathbf{A}_S \mathbf{x} + \mathbf{B}_S \mathbf{u} \\ \mathbf{y} &= \mathbf{C}_S \mathbf{x} + \mathbf{D}_S \mathbf{u} \end{aligned} \quad (19)$$

where

$$\mathbf{x} = [\mathbf{x}_1 \ \mathbf{x}_2 \ \mathbf{x}_3 \ \mathbf{x}_4]_{4N \times 1}^T = [\mathbf{q} \ \dot{\mathbf{q}} \ \tilde{\mathbf{i}}_L \ \mathbf{i}_L]_{4N \times 1}^T,$$

$$\mathbf{u} = [\mathbf{f}_d]_{N \times 1},$$

$$\mathbf{A}_S = \begin{bmatrix} \mathbf{0} & \mathbf{I} & \mathbf{0} & \mathbf{0} \\ -\mathbf{M}^{-1}\mathbf{K} & -\mathbf{M}^{-1}\mathbf{C} & -\mathbf{M}^{-1}\mathbf{B}_R & -\mathbf{M}^{-1}\mathbf{B}_L \\ \mathbf{0} & \mathbf{0} & \mathbf{0} & \mathbf{I} \\ -\Psi & \mathbf{0} & -\Gamma & -\Omega \end{bmatrix}_{4N \times 4N},$$

$$\mathbf{B}_S = \begin{bmatrix} \mathbf{0} \\ \mathbf{M}^{-1} \\ \mathbf{0} \\ \mathbf{0} \end{bmatrix}_{4N \times N},$$

$$\mathbf{C}_S = [\mathbf{C}_1 \ \mathbf{0} \ \mathbf{0} \ \mathbf{0}]_{1 \times 4N}, \quad \mathbf{D}_S = [\mathbf{0}]_{1 \times N}.$$

$\mathbf{C}_1 = \left[\sin \frac{\pi x_d}{L} \ \dots \ \sin \frac{N\pi x_d}{L} \right]_{1 \times N}$ is formed by

choosing the response measured at middle of beam, $x_d = L/2$, resulting in $\phi_r(x_d) = \sin(r\pi x_d/L)$ ($r = 1, \dots, N$).

5 A numerical example

Assume $\phi_r(x) = \sin(r\pi x/L)$ ($r = 1, \dots, N$) which satisfies all boundary conditions (Hinged-Hinged), obtained

For $s = r$,

$$m_{rr} = \frac{\rho_b A_b L + \rho_p A_p (x_2 - x_1)}{2} + \frac{\rho_p A_p L}{2\pi r} \left[\sin\left(\frac{2\pi r x_1}{L}\right) - \sin\left(\frac{2\pi r x_2}{L}\right) \right],$$

$$k_{rr} = \left(\frac{r\pi}{L}\right)^4 \left\{ \frac{E_b I_b L + E_p I_p (x_2 - x_1)}{2} + \frac{E_p I_p L}{2\pi r} \left[\sin\left(\frac{2\pi r x_1}{L}\right) - \sin\left(\frac{2\pi r x_2}{L}\right) \right] \right\},$$

For $s \neq r$,

$$m_{sr} = \frac{\rho_p A_p L}{\pi(r^2 - s^2)} \left(r \sin \frac{s\pi x_1}{L} \cos \frac{r\pi x_1}{L} - s \sin \frac{r\pi x_1}{L} \cos \frac{s\pi x_1}{L} - r \sin \frac{s\pi x_2}{L} \cos \frac{r\pi x_2}{L} + s \sin \frac{r\pi x_2}{L} \cos \frac{s\pi x_2}{L} \right),$$

$$k_{sr} = \frac{E_p I_p L}{(r^2 - s^2)\pi} \left(\frac{rs\pi^2}{L^2} \right)^2 \left(r \sin \frac{s\pi x_1}{L} \cos \frac{r\pi x_1}{L} - s \sin \frac{r\pi x_1}{L} \cos \frac{s\pi x_1}{L} - r \sin \frac{s\pi x_2}{L} \cos \frac{r\pi x_2}{L} + s \sin \frac{r\pi x_2}{L} \cos \frac{s\pi x_2}{L} \right),$$

$$B_S^L = \frac{h_{31} h_p (2h_b + h_p) s \pi L_S}{2(x_2 - x_1) L R_S} \left[\cos\left(\frac{s\pi x_1}{L}\right) - \cos\left(\frac{s\pi x_2}{L}\right) \right],$$

$$B_S^R = \frac{h_{31} h_p (2h_b + h_p) s \pi}{2(x_2 - x_1) L} \left[\cos\left(\frac{s\pi x_1}{L}\right) - \cos\left(\frac{s\pi x_2}{L}\right) \right],$$

$$\psi_r = \frac{h_{31} h_p (2h_b + h_p) r \pi}{2(x_2 - x_1) L} \left[\cos\left(\frac{r\pi x_1}{L}\right) - \cos\left(\frac{r\pi x_2}{L}\right) \right].$$

Given a beam and a PZT, the parameters are,

Beam:

$$V_b = 0.5 \times 0.025 \times 0.003 \text{ (m}^3\text{)}, \quad \rho_b = 2700 \text{ (Kg/m}^3\text{)}, \\ E_b = 70 \text{ (GPa)}, \quad \alpha = 0.2, \quad \gamma = 10^{-7}, \quad x_d = 0.25 \text{ (m)}.$$

PZT:

$$V_p = 0.06 \times 0.025 \times 0.00025 \text{ (m}^3\text{)},$$

$$x_1 = 0.22 \text{ (m)}, \quad x_2 = 0.28 \text{ (m)},$$

$$E_p = 70 \text{ (GPa)}, \quad h_{31} = 7 \times 10^7 \text{ (N/C)}, \quad C_p = 50 \text{ (nF)},$$

Shunt circuit components to target the first mode:

$$L_1 = 602 \text{ (H)}, \quad R_1 = 300 \text{ (k}\Omega\text{)}.$$

After solving the state space equation (19) with MATLAB®, the impulse responses of with and without parallel RL piezoelectric shunt control are shown in Figure 3 where there are three frequency components ($N = 3$), the first mode frequency measured is $f_1 = 29$ Hz.

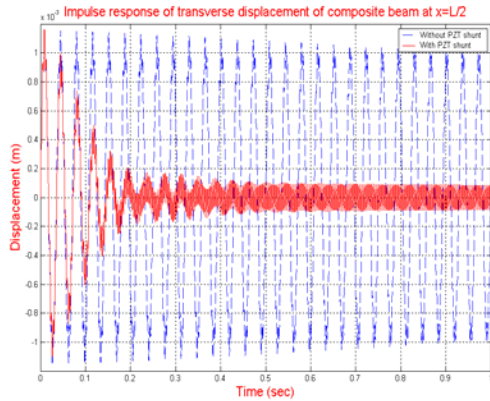


Figure 3 Impulse response of beam (a) without shunt control (constant large amplitudes), (b) with shunt control (Amplitudes rapidly decreasing)

Figure 3 shows that the vibration amplitude of the beam is significantly reduced when the inductor of shunt circuit is tuned to the frequency to be controlled, that is:

$$L_1 = \frac{1}{(2\pi f_1)^2 C_p}$$

When the shunt circuit is ill-tuned, the control will become worse.

6 Simulation results of passive piezoelectric vibration shunt with ANSYS®

A method of passive vibration shunt control modeling using Finite Element Analysis (FEA) software package ANSYS® has been developed [5]. The simulation of parallel R-L shunt control on an aluminum beam showed that 1st to 4th modes of vibration amplitudes were reduced by 84%, 70%, 80%, and 92% respectively. However, it was found that control effectiveness was dramatically worsened when the beam material was changed to wood. Simulation results showed that little amplitude drop at natural frequency for a wooden beam that has Young's modulus $E_b = 6.67$ (GPa), and density $\rho_b = 535$ (Kg/m³) respectively. This is due to the Young's modulus of wood are much smaller than that of PZT. Since the more strain energy PZT gets, the more vibration energy it can remove. Here, the strain energy transfer between beam and PZT is discussed.

7 Results with different material properties

The above simulation results have shown that the vibration amplitude of aluminum beam at natural frequencies can be significantly reduced. However, simulation has shown that the results are dramatically worsened when the beam material is changed to wood. Figure 6 displays the vibration spectrum of a wooden beam which Young's modulus is equal to, and density is equal to $\rho_b = 535$ (Kg/m³). The results show that little amplitude has been reduced at natural frequencies. This is probably because the Young's modulus and the density of the wood are much smaller than that of the PZT ceramic.

In order to improve the efficiency of vibration shunting, a joint beam was constructed shown in Figure 4. The left section is wooden material, right section is a composite material which Young's modulus is equal to $E_b = 66$ (GPa), and density is equal to $\rho_b = 600$ (Kg/m³). The PZT patch was attached on the top of composite material beam.

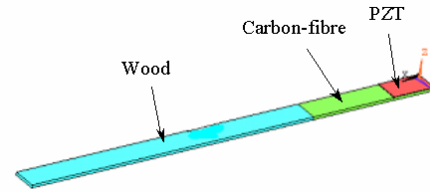


Figure 4 Joint beam with PZT patch attached

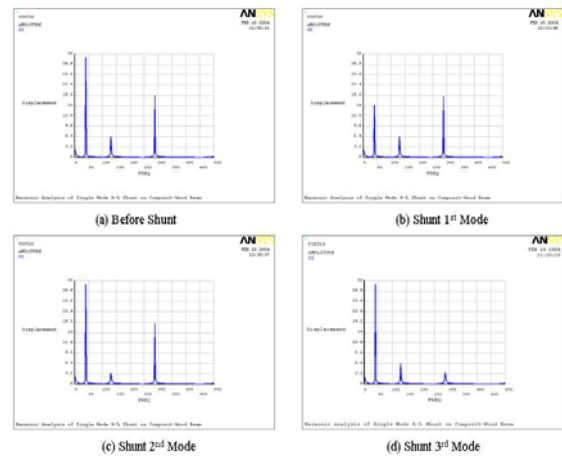


Figure 5 Harmonic analysis of joint beam vibration

Figure 5 is the simulation results of the joint beam. It shows that reduction of the vibration amplitude at natural frequency is markedly improved. 1st to 3rd modes were reduced about 48%, 50%, and 80% (or 5.68 dB, 6 dB, and 14 dB) respectively. The

vibration shunt has been improved by using composite material instead of the wood material. The composite material has its flexibility. The Young's modulus of composite material can be specifically chosen by the designer during its fabrication.

8 Strain energy in the PZT layer

The neutral axis of a composite beam with PZT attached is determined by the Young's modulus as well as the thickness of the two materials. Figure 6 depicts the cross-sectional area of the composite beam. The dash line indicates the position of the neutral axis that is calculated by,

$$\bar{z} = \frac{A_b E_b z_b + A_p E_p z_p}{A_b E_b + A_p E_p} = \frac{h_b (\mu^2 n + 2\mu + 1)}{2(1 + \mu n)} \quad (20)$$

where

$$\mu = \frac{h_p}{h_b} \text{ is the thickness ratio of PZT to beam.}$$

$$n = \frac{E_p}{E_b} \text{ is the Young's modulus ratio of PZT to beam.}$$

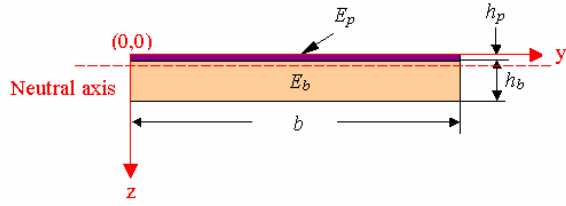


Figure 6 Cross-sectional area of the composite beam

Since the axial strain $\varepsilon_{11} = -z \frac{\partial^2 w}{\partial x^2}$, it is proportional to the distance from neutral axis "z". When n is very large, that is the Young's modulus of PZT is much larger than that of structure (in the case of PZT attached on wood), the neutral axis will be very close to the centroid of the PZT that will reduce the axial strain and might reduce the strain energy transferred to PZT. The average strain, the strain in the middle (centroid) surface of the PZT is

$$\begin{aligned} (\varepsilon_p)_{Ave} &= -\frac{M(z_p - \bar{z})}{E_b I_b + E_p I_p} = \frac{M(\bar{z} - z_p)}{E_b (I_b + n I_p)} \\ &= \left(\frac{6M}{bh_b^2 E_b} \right) \frac{\mu + 1}{\mu^4 n^2 + (4\mu^3 + 6\mu^2 + 4\mu)n + 1} \quad (21) \end{aligned}$$

where

$$z_p = h_p / 2$$

The plot of the average strain in the PZT with four different thickness ratios is shown in Figure 7. The

Young's modulus of the beam and bending moment used in the simulation are $E_b = 7 \text{ (GPa)}$ and $M = 100 \text{ (N-m)}$ respectively.

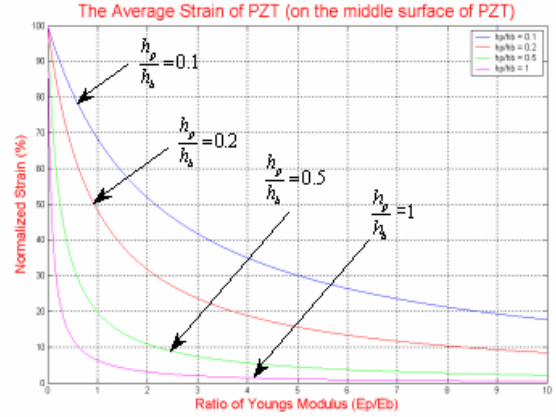


Figure 7 Average strain of the PZT layer

The h -form constitutive relation of piezoelectric materials (IEEE 1987) is

$$\begin{cases} \sigma = E_p \varepsilon - hD \\ E = -h\varepsilon + \beta D \end{cases} \quad (22)$$

where

E — Electrical field (V/m)

E_p — Young's modulus of PZT (N/m^2 or Pa)

β — Dielectric impermeability (m/F or $V\text{-}m/C$)

D — Electrical displacement (C/m^2)

ε — Mechanical strain

h — Electrical field-strain coefficient of PZT (V/m or N/C)

Reorganizing the top part of equation (22),

$$\sigma = E_p \varepsilon - hD = E'_p \varepsilon \quad (23)$$

Therefore,

$$D = \frac{E_p - E'_p}{h} \varepsilon \quad (24)$$

If $D = 0$, $E'_p = E_p$, which is the Young's modulus without considering electrical field or the electrodes of the PZT at short circuit.

Substituting equation (24) into the second equation of the equation (22) obtains

$$E = -h\varepsilon + \beta \frac{E_p - E'_p}{h} \varepsilon = \left(\frac{\beta(E_p - E'_p)}{h} - h \right) \varepsilon \quad (25)$$

Equation (25) indicates that the electrical field E produced in the PZT is in proportion to its strain ε . Larger strain will produce larger electrical field thus

larger output voltage. Therefore, more mechanical energy can be converted into electrical energy that can be dissipated by an electrical network.

For example, given a composite beam which has thickness ratio $\mu = 0.1$, from Figure 7, it can be seen that the average strain for $n = 10$ is about one-quarter of that for $n = 1$. This is the reason why the vibration reduction for the wooden beam is much less than the reduction for the aluminium or carbon-fibre beam using the passive piezoelectric vibration shunt control method.

9 Experimental Results

In work already submitted for review [6], it demonstrated that the vibration reduction could be more efficient by reducing the difference between the Young's Modulus of the structure to be controlled and that of for the PZT. For example, 80% reduction in the amplitude of vibration is observed for the PZT-Carbon-fiber combination when compared to 8% for the PZT-wood combination

10 Conclusions

An analytical study on the parallel resistor-inductor piezoelectric shunt control has been presented. Material properties (Mechanical and physical) of the structure to be controlled can significantly affect the shunt control ability as a result of the neutral axis location. The analysis has shown that the Young's modulus ratio between the PZT patch and structure can influence the strain energy transfer onto the PZT patch thus it affects efficiency of the vibration shunt control since the electrical field produced in the PZT is in proportion to its strain. Larger strain will result in a larger electrical field, thus larger output voltage. When the shunt control is applied to the carbon-fiber structure, it can achieve good control efficiency. Simulation and experimental results have verified the impact of material property variations. The results are corroborated from analytical, experimental and computational analyses.

Acknowledgements

This work is co-supported by an Australian Research Council (ARC) grant (Grant number LP 0222482).

References

- [1] N. W. Hagood and A. von Flotow, "Damping of Structural Vibrations with Piezoelectric Materials and Passive Electrical Networks", *Journal of Sound and Vibration*, 146(2), pp. 243 – 268, 1991.
- [2] D. L. Edberg, A. S. Bicos, C. M. Fuller, J. J. Tracy and J. S. Fechter, "Theoretical and Experiment Studies of a Truss Incorporating

Active Members", *J. Intell. Mater. Syst. and Struct.*, 3, 444, 1992.

- [3] S. Y. Wu, "Piezoelectric Shunts with a Parallel R-L Circuit for Structural Damping and Vibration Control", *Proceedings of the International Society for Optical Engineering*, Vol. 2720, pp. 259 – 269, 1996.
- [4] K. W. Wang, J. S. Lai and W. K. Yu, "An energy-based parametric control approach for structural vibration suppression via semi-active piezoelectric networks", *Journal of vibration and acoustics*, Vol. 118, pp. 505 – 509, 1996.
- [5] Cao J L, John S, and Molyneaux T, "Finite element analysis modeling of piezoelectric shunting for passive vibration control", *Int. Conf. on Computational Intelligence for Modeling Control and Automation – CIMCA'2004*, 12–14 July 2004, Gold Coast, Australia, pp 817-825, ISBN 174 0881885..
- [6] Cao J L, John S and Molyneaux T, "Piezoelectric-based vibration control optimization in nonlinear composite structures", *12th SPIE Annual Int. Symp. on Smart Struct. and Mater.*, 6–10 March 2005, San Diego, California USA.